

UC Irvine

UC Irvine Previously Published Works

Title

Intestinal Phospholipid Remodeling Is Required for Dietary-Lipid Uptake and Survival on a High-Fat Diet

Permalink

<https://escholarship.org/uc/item/8bj647t6>

Journal

Cell Metabolism, 23(3)

ISSN

1550-4131

Authors

Wang, Bo

Rong, Xin

Duerr, Mark A

et al.

Publication Date

2016-03-01

DOI

10.1016/j.cmet.2016.01.001

Copyright Information

This work is made available under the terms of a Creative Commons Attribution License, available at <https://creativecommons.org/licenses/by/4.0/>

Peer reviewed

Intestinal Phospholipid Remodeling Is Required for Dietary-Lipid Uptake and Survival on a High-Fat Diet

Bo Wang,^{1,2} Xin Rong,^{1,2} Mark A. Duerr,⁴ Daniel J. Hermanson,⁵ Per Niklas Hedde,^{6,7} Jinny S. Wong,⁸ Thomas Q. de Aguiar Vallim,³ Benjamin F. Cravatt,⁵ Enrico Gratton,^{6,7} David A. Ford,⁴ and Peter Tontonoz^{1,2,*}

¹Department of Pathology and Laboratory Medicine

²Howard Hughes Medical Institute

³Division of Cardiology, Department of Medicine

University of California, Los Angeles, Los Angeles, CA 90095, USA

⁴Department of Biochemistry and Molecular Biology, Center for Cardiovascular Research, Saint Louis University, St. Louis, MO 63104, USA

⁵Department of Chemical Physiology, The Skaggs Institute for Chemical Biology, The Scripps Research Institute, La Jolla, CA 92037, USA

⁶Laboratory of Fluorescence Dynamics, Biomedical Engineering Department

⁷Center for Complex Biological Systems

University of California, Irvine, Irvine, CA 92697, USA

⁸Electron Microscopy Core, Gladstone Institute of Cardiovascular Disease, San Francisco, CA 94158, USA

*Correspondence: ptontonoz@mednet.ucla.edu

<http://dx.doi.org/10.1016/j.cmet.2016.01.001>

SUMMARY

Phospholipids are important determinants of membrane biophysical properties, but the impact of membrane acyl chain composition on dietary-lipid absorption is unknown. Here we demonstrate that the LXR-responsive phospholipid-remodeling enzyme *Lpcat3* modulates intestinal fatty acid and cholesterol absorption and is required for survival on a high-fat diet. Mice lacking *Lpcat3* in the intestine thrive on carbohydrate-based chow but lose body weight rapidly and become moribund on a triglyceride-rich diet. *Lpcat3*-dependent incorporation of polyunsaturated fatty acids into phospholipids is required for the efficient transport of dietary lipids into enterocytes. Furthermore, loss of *Lpcat3* amplifies the production of gut hormones, including GLP-1 and oleoylethanolamide, in response to high-fat feeding, contributing to the paradoxical cessation of food intake in the setting of starvation. These results reveal that membrane phospholipid composition is a gating factor in passive lipid absorption and implicate LXR-*Lpcat3* signaling in a gut-brain feedback loop that couples absorption to food intake.

INTRODUCTION

Phospholipid composition is an important determinant of membrane biophysical properties. It is therefore reasonable to hypothesize that changes in the incorporation of polyunsaturated acyl chains into phospholipids might impact lipid transport across cellular membranes. However, it has heretofore been difficult to test this idea, as experimental systems that

would allow selective alteration of phospholipid abundance in living animals have not been available. It has been speculated that reduced abundance of the essential fatty acid (EFA) linoleate in intestinal membranes may be linked to malabsorption (Clark et al., 1973; Werner et al., 2002). EFA deficiency was reported to be associated with fat malabsorption in the 1940s (Barnes et al., 1941), but the underlying mechanisms have remained obscure. Studies have suggested that defects in one or more intracellular events, including fatty acid (FA) uptake, triglyceride (TG) re-esterification, and chylomicron secretion, may contribute to reduced fat absorption in EFA deficiency (Clark et al., 1973; Levy et al., 1992; Werner et al., 2002). But how the loss of EFAs may affect these processes is unknown. To date, the hypothesis that altered membrane composition could affect lipid absorption *in vivo* has not been tested.

It has long been debated whether FAs are transported across the enterocyte apical membrane via passive diffusion or by carrier-mediated processes (Tso et al., 2004). Several candidate FA transporters have been characterized, including FATP4 and CD36 (Harmon et al., 1992; Stahl et al., 1999; Tso et al., 2004). Although conflicting results have been reported, deletion of either CD36 or FATP4 alone in mouse intestine does not appear to dramatically alter FA uptake (Goudriaan et al., 2002; Nauli et al., 2006; Shim et al., 2009). Studies utilizing cultured cell systems have supported a passive diffusion model by showing that the rate of FA uptake is linear, protease resistant, and temperature independent (Chow and Hollander, 1979; Ling et al., 1989; Trotter et al., 1996). By contrast, others have pointed to a carrier-mediated model based on observations that FA uptake is saturable and competitive with other FAs (Ho and Storch, 2001; Murota and Storch, 2005). While the preponderance of *in vitro* data supports a principal role for diffusion, testing the contribution of passive diffusion *in vivo* has been difficult due to the lack of an appropriate model system. No genetic mutation has been reported that directly affects passive FA uptake in animals.

We recently identified a nuclear receptor pathway for dynamic modulation of membrane phospholipid composition in response to changes in cellular lipid metabolism (Rong et al., 2013). Ligand activation of liver X receptors (LXRs) preferentially drives the incorporation of polyunsaturated FAs into phospholipids through induction of the remodeling enzyme lysophosphatidylcholine acyltransferase 3 (Lpcat3). Loss of Lpcat3 in liver selectively reduces arachidonoyl phosphatidylcholine (PC) in liver membranes, leading to decreased membrane fluidity and curvature and impaired VLDL secretion (Rong et al., 2015; Hashidate-Yoshida et al., 2015). The ability to regulate Lpcat3 activity has provided an unprecedented opportunity to test the physiologic consequences of changing membrane phospholipid composition in vivo.

Here we demonstrate that Lpcat3 deficiency in the intestine leads to a selective defect in the ability to incorporate the EFAs linoleate and arachidonate into phospholipids. We further show that this deficiency leads to marked changes in the biophysical properties of intestinal membranes and impairs passive FA transport into enterocytes and chylomicron production. Lpcat3 deficiency in the setting of a TG-rich diet leads to the exacerbated production of gut hormones and the cessation of food intake despite starvation. These data provide direct evidence for the critical importance of membrane phospholipid acyl chain composition in gating passive dietary-lipid uptake and determining feedback responses to ingestion of a lipid-rich diet.

RESULTS

Loss of Lpcat3 in Intestine Decreases Plasma-TG and Cholesterol Levels

We previously reported that mice deficient in Lpcat3 expression in the intestine (herein referred to as Lpcat3 IKO or IKO mice) showed severe post-natal growth retardation and failure to thrive (Rong et al., 2015). Surprisingly, however, we found that a minority of the pups could survive until weaning. Furthermore, once the surviving pups were weaned onto chow diet (13.5% calories from fat, 0.02% cholesterol) at 4 weeks of age, they grew rapidly and ultimately reached a similar size as their littermates (Figure 1A). Analysis of plasma lipid levels revealed lower serum TG and total cholesterol levels in Lpcat3 IKO mice compared to Lpcat3-floxed, Cre-negative controls (Figure 1B). There was no difference in plasma nonesterified free fatty acid (NEFA) levels between groups. Blood glucose levels were slightly lower in the knockout (KO) mice. Fractionation of plasma lipoproteins showed lower levels of TG in the very-low-density lipoprotein (VLDL) fraction, and cholesterol in high-density lipoprotein (HDL) fraction, in Lpcat3 IKO mice (Figure 1C).

Unexpectedly, and in contrast to our observations in suckling 1-week-old pups (Rong et al., 2015), we did not observe lipid accumulation in enterocytes of adult IKO mice (Figure 1D). Rather, we observed hypertrophy of mucosal villi in the duodenum and jejunum. Each villus contained multiple distorted branches, consistent with compensatory enlargement of the absorptive surface (Skála and Konrádová, 1969). In line with the hypertrophy of villi, the small intestine was significantly longer in Lpcat3 IKOs than in controls (Figure 1E). We previously reported that Lpcat3 is an LXR target in liver and intestine (Rong et al., 2015). We found that intestinal Lpcat3 expression is also

regulated by the FA sensor peroxisome proliferator-activated receptor δ (PPAR δ). Administration of GW742 (a potent PPAR δ agonist) to mice increased Lpcat3 expression in the intestine (Figure 1F).

Lpcat3 Is Required for Survival on a HFD or Western Diet

Since Lpcat3 IKO pups showed severe growth retardation and lethality when suckling on lipid-rich milk (Rong et al., 2015), we tested how adult mice responded to diets rich in fat. We first fed mice a high-fat diet (HFD; 60% calories from fat, 0.028% cholesterol) starting at 8–10 weeks of age—a time at which floxed control and Lpcat3 IKO mice were of similar body weight. Surprisingly, Lpcat3 IKO mice lost ~20% of their body weight within 10 days and became moribund, necessitating termination of the study (Figure 2A). Similar rapid weight loss and failure to thrive were also observed in Lpcat3 IKO mice on a western diet (40% calories from fat, 0.2% cholesterol; Figure 2B). IKO mice lost ~20% of their body weight after 1 week of feeding, and one mouse died on day 4. Interestingly, the decline of Lpcat3 IKO mice on HFD or western diet was reversible. Lpcat3 IKO mice fed HFD recovered their body weight within 2 days when switched back to chow diet (Figure 2C). Furthermore, there was no difference in weight loss between HFD- and western-diet-fed IKO mice (Figure 2D), indicating that the TG, rather than the cholesterol, content of the western diet is the primary cause of weight loss. IKO mice actually gained slightly more weight when fed a high-cholesterol diet (13.5% calories from fat, 1.25% cholesterol) compared to controls (Figure S1A, available online).

MRI analysis of body composition showed that the weight loss after HFD or western-diet feeding was primarily due to loss of body fat (Figure 2E). Remarkably, blood glucose levels in both HFD- and western-diet-fed Lpcat3 IKO mice were markedly lower than those in control mice (Figure 2F). Intestinal morphology in high-fat-fed IKO mice was similar to that of chow-diet-fed Lpcat3 IKO mice, with hypertrophy of villi and the absence of lipid accumulation in enterocytes (Figure 2G). Compared to control mice, there was no difference in the infiltration of inflammatory cells into the intestine of IKO mice fed a HFD. Moreover, there was no difference in the expression of inflammatory cytokines or chemokine receptors between control and IKO intestine (Figure 2H). These findings suggest that the weight loss is not due to acute induction of intestinal inflammation in response to HFD. Interestingly, the livers of Lpcat3 IKO mice showed steatosis. Coupled with the finding of hypoglycemia, this observation suggested that the Lpcat3 IKO mice were starving. Gene expression analysis revealed significant reduction in the expression of *Ppara* and genes involved in FA oxidation (Figure S1B), a finding consistent with reduced FA availability in the liver.

Lpcat3 Deficiency Reduces Food Intake on HFD through GLP-1 Induction

Next, we sought to understand the cause of the striking weight loss in IKO mice fed HFD. We first monitored daily food consumption in individually housed mice. Although Lpcat3 IKO mice consumed a similar amount of food to that of controls when fed chow diet (Figure 3A), they ate less than half as much as controls upon switching to 60% HFD or western diet

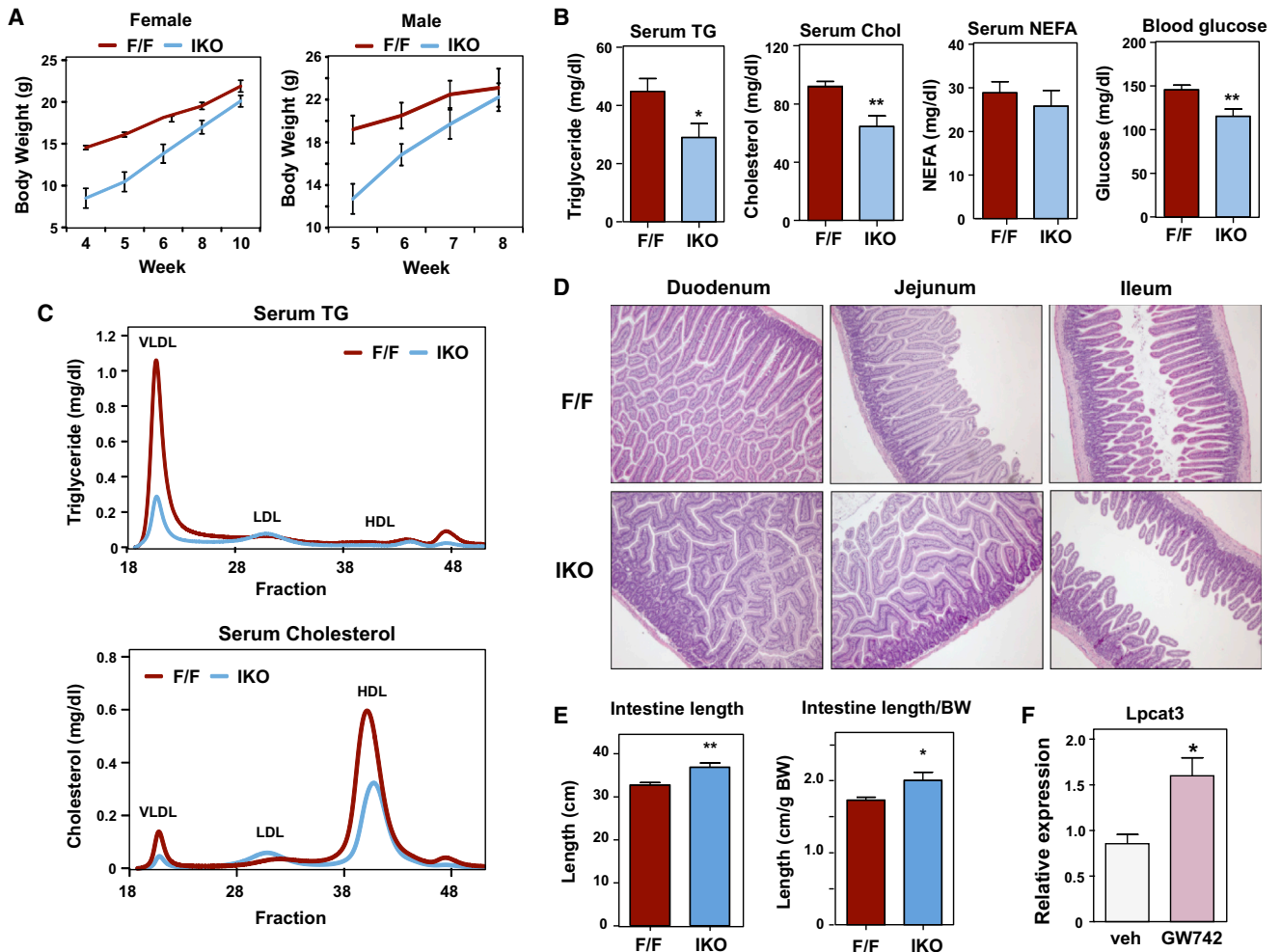


Figure 1. Reduced Plasma-TG and Cholesterol Levels in Intestine-Specific *Lpcat3* Knockout Mice

(A) Growth curve of *Lpcat3*^{fl/fl} (F/F) and *Lpcat3*^{fl/fl} Villin-Cre (IKO) mice on chow diet after weaning ($n \geq 6$ /group).

(B) Plasma lipid and glucose levels in 8- to 10-week-old chow-diet-fed *Lpcat3*^{fl/fl} (F/F) and *Lpcat3*^{fl/fl} Villin-Cre (IKO) mice ($n \geq 6$ /group). Mice were fasted for 6 hr before blood collection.

(C) Lipoprotein profiles of *Lpcat3*^{fl/fl} (F/F) and *Lpcat3*^{fl/fl} Villin-Cre (IKO) mice. Plasma from F/F and IKO mice was pooled ($n = 5$) and analyzed by fast protein liquid chromatography (FPLC).

(D) Hematoxylin and eosin (H&E) staining of intestine sections from *Lpcat3*^{fl/fl} (F/F) and *Lpcat3*^{fl/fl} Villin-Cre (IKO) mice.

(E) Small intestine length of *Lpcat3*^{fl/fl} (F/F) and *Lpcat3*^{fl/fl} Villin-Cre (IKO) mice ($n \geq 6$ /group).

(F) Induction of *Lpcat3* mRNA expression in intestines of mice treated with 20 mg/kg/day GW742 by oral gavage for 5 days ($n = 5$ /group). Gene expression was measured by real-time PCR.

Values are means \pm SEM. Statistical analysis was performed with Student's *t* test. * $p < 0.05$; ** $p < 0.01$.

(Figures 3B and S2A). To determine if the reduced food intake was the sole cause of weight loss in *Lpcat3*-deficient mice, we performed a pair-feeding study. As shown in Figure 3C, control mice limited to the same amount of HFD consumed by the IKO mice lost $\sim 7\%$ of their body weight within 1 week, compared to $\sim 17\%$ for the *Lpcat3* IKO mice. Body-fat composition in *Lpcat3* IKO after 1 week was 5%, compared to 10% in pair-fed controls (Figure S2B). These observations indicated that reduced food intake was a contributor to, but not the only cause of, weight loss in IKO mice. Blood glucose levels were comparably reduced in *Lpcat3* IKO and pair-fed controls (Figure 3D), suggesting that the hypoglycemia of IKO mice was largely due to starvation.

Next, we investigated the etiology of reduced food consumption in *Lpcat3*-deficient mice. We fasted mice overnight, offered them both HFD and chow diet, and monitored their food preference for 24 hr. Interestingly, both control and IKO mice preferred the HFD and consumed the same amount of HFD during the first 2 hr (Figure 3E). After 2 hr, control mice continued to eat almost exclusively HFD and consumed only a minimal amount of chow. By contrast, the IKO mice stopped eating after the first 2 hr and consumed neither diet. No difference in food intake was observed when the mice were refed with chow diet in a similar experiment (Figure S2C). Surprisingly, the IKO mice actually consumed slightly more food on high-cholesterol diet (Figure S2D). These observations suggested that dietary fat was

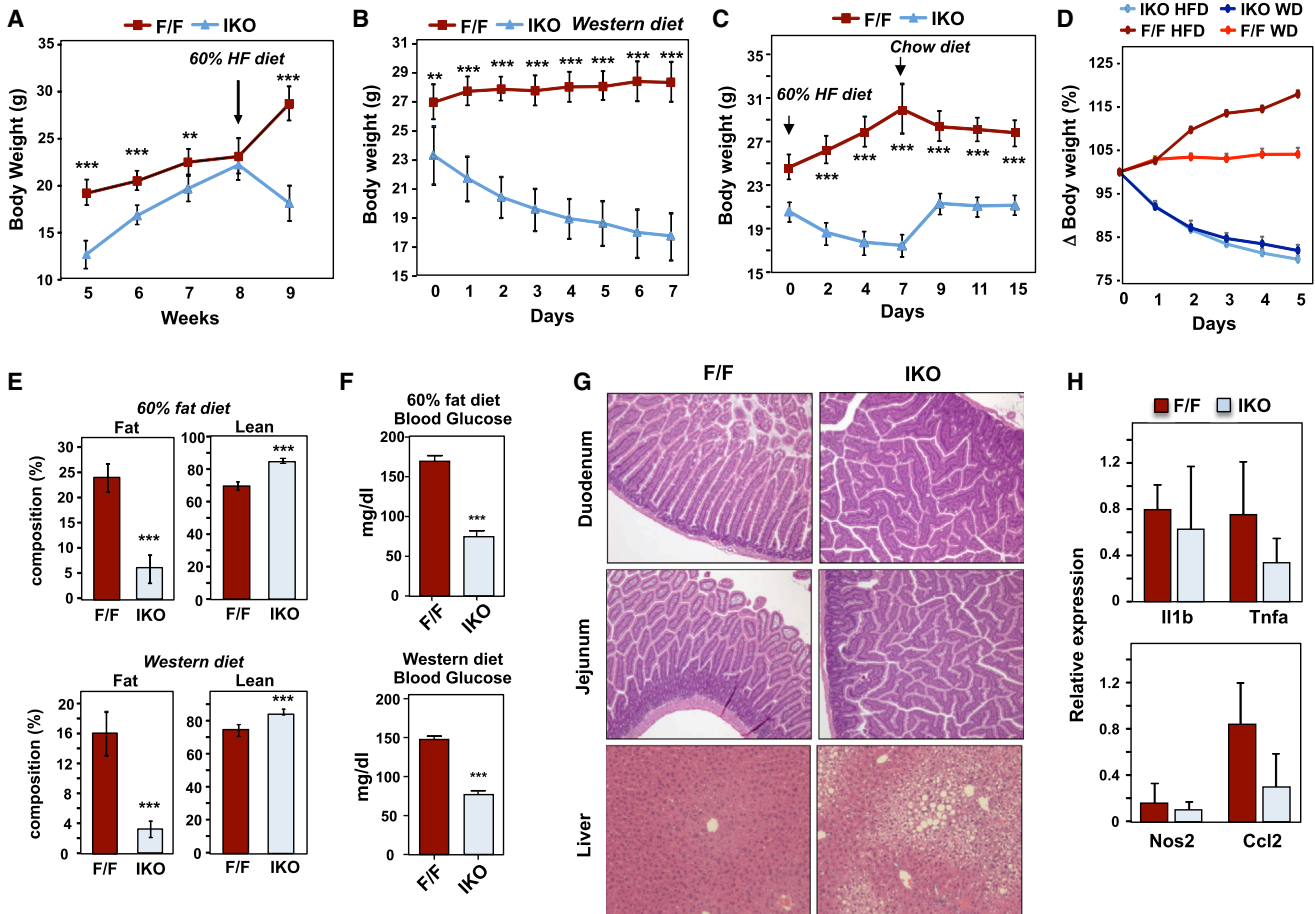


Figure 2. Mice Lacking *Lpcat3* Cannot Survive on HFD or Western Diet

(A and B) Growth curve of male *Lpcat3^{fl/fl}* (F/F) and *Lpcat3^{fl/fl} Villin-Cre* (IKO) mice placed on chow diet after weaning and then switched to 60% HFD (A) ($n \geq 6$ /group) or western diet (B) ($n \geq 4$ /group).

(C) Growth curve of female *Lpcat3^{fl/fl}* (F/F) and *Lpcat3^{fl/fl} Villin-Cre* (IKO) mice on 60% HFD for 7 days and switched back to chow diet ($n \geq 4$ /group).

(D) Body-weight change in 60% HFD- and western-diet-fed mice ($n \geq 4$ /group).

(E) Body composition of *Lpcat3^{fl/fl}* (F/F) and *Lpcat3^{fl/fl} Villin-Cre* (IKO) mice on 60% HFD for 10 days ($n \geq 6$ /group) and western diet for 8 days ($n \geq 4$ /group).

(F) Blood glucose levels in *Lpcat3^{fl/fl}* (F/F) and *Lpcat3^{fl/fl} Villin-Cre* (IKO) mice on 60% HFD and western diet as in (D).

(G) H&E staining of intestine and liver sections from *Lpcat3^{fl/fl}* (F/F) and *Lpcat3^{fl/fl} Villin-Cre* (IKO) mice on 60% HFD for 10 days.

(H) Expression of inflammatory genes in fasting and 60% HFD-refed intestines measured by real-time PCR ($n \geq 4$ /group).

Values are means \pm SEM. Statistical analysis was performed with two-way ANOVA (A–D) and Student's *t* test (E, F, and H). * $p < 0.05$, ** $p < 0.01$, *** $p < 0.001$.

inhibiting total food intake in *Lpcat3* IKO mice, regardless of the type of food offered.

Previous studies have identified gut-derived hormones that are induced by dietary fat, including GLP-1, PYY, and CCK (Begg and Woods, 2013; Camilleri, 2015). To determine whether any of these mediators were in play in *Lpcat3*-deficient mice, we measured their levels in the plasma of high-fat-fed mice. Remarkably, active GLP-1 levels were 6-fold higher, and PYY levels were 3-fold higher in *Lpcat3* IKO mice compared to controls (Figure 3F). There was no difference in CCK levels. Interestingly, GLP-1 levels were also increased by 3-fold in chow-diet-refed IKO mice, while PYY levels were not changed (Figure S2E). To test whether this induction of GLP-1 was contributing to the reduction in food intake, we injected mice with the GLP-1 receptor antagonist exendin-(9–39) (Ex-9) and

monitored food intake during fasting/refeeding. Compared to vehicle treatment, Ex-9 treatment increased HFD consumption in IKO mice to similar levels as control mice during the first 6 hr (Figure S2F). Similarly, chronic Ex-9 treatment over the course of 4 days partially rescued food intake and weight loss in HFD-fed IKO mice (Figures 3G and S2G). These findings indicate that excessive GLP-1 signaling contributes to the food intake phenotype of *Lpcat3*-deficient mice.

The partial rescue of food intake by GLP-1 receptor antagonist indicates that additional anorexic pathways are also involved. N-acylphosphatidylethanolamine (NAPE) and oleoylethanolamide (OEA) are induced by fat digestion and inhibit food intake through interactions with the CNS (Gillum et al., 2008; Fu et al., 2003; Schwartz et al., 2008). The endocannabinoids, anandamide (AEA) and 2-arachidonoyl glycerol (2-AG), increase food

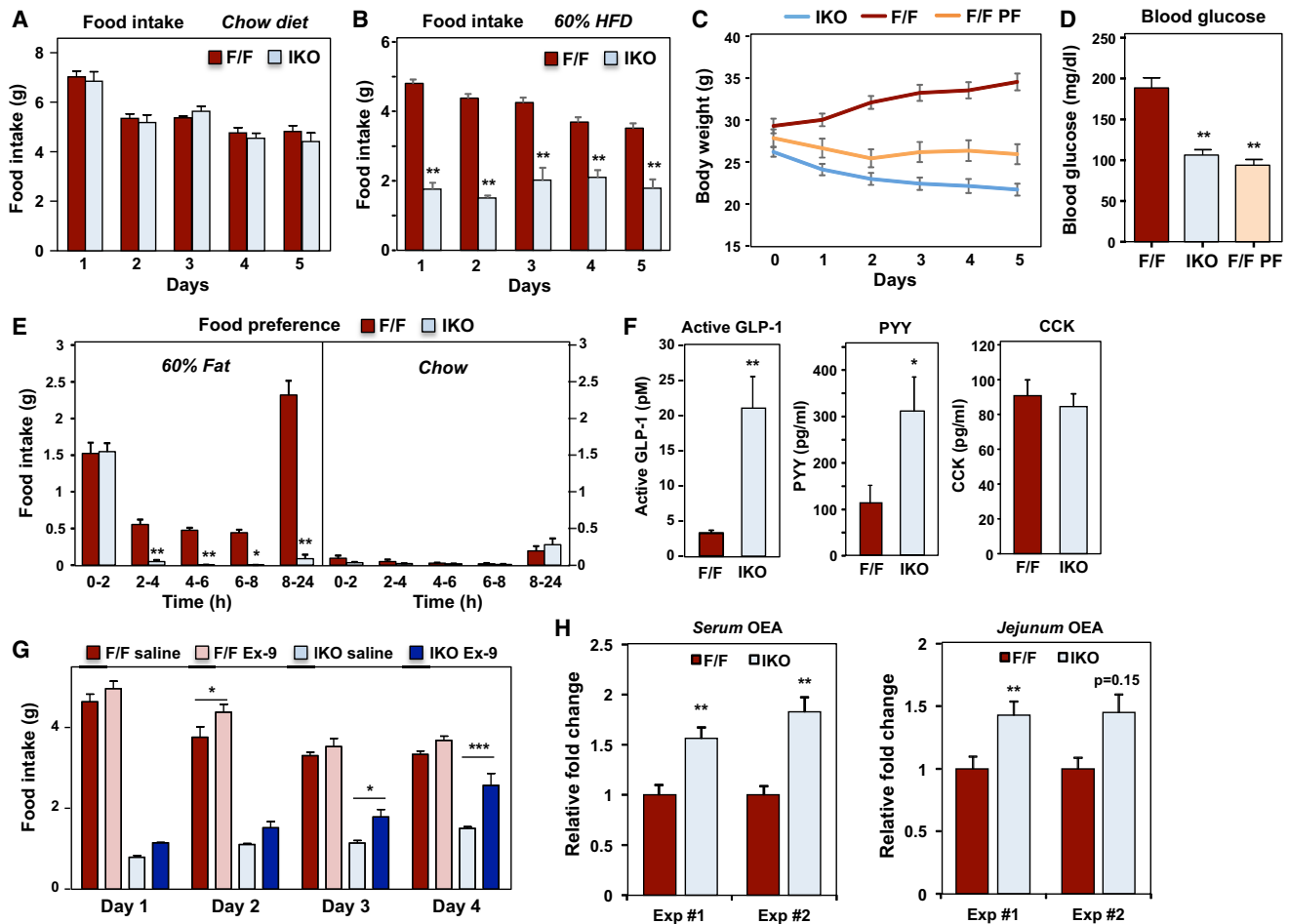


Figure 3. TG-Rich Diets Inhibit Feeding in *Lpcat3* IKO Mice

(A and B) Daily food intake in male *Lpcat3*^{fl/fl} (F/F) and *Lpcat3*^{fl/fl} Villin-Cre (IKO) mice on chow diet (A) and 60% HFD (B).

(C) Growth curve of male *Lpcat3*^{fl/fl} (F/F), *Lpcat3*^{fl/fl} Villin-Cre (IKO), and pair-feeding *Lpcat3*^{fl/fl} (F/F PF) mice ($n \geq 5$ /group).

(D) Blood glucose levels in mice in (C).

(E) Food preference test in female *Lpcat3*^{fl/fl} (F/F) and *Lpcat3*^{fl/fl} Villin-Cre (IKO) during fasting/refeeding. Mice were fasted overnight and provided with both 60% HFD and chow diet. Food intake was monitored for 24 hr ($n \geq 5$ /group).

(F) ELISA analysis of active GLP-1, PYY, and CCK in the plasma of *Lpcat3*^{fl/fl} (F/F) and *Lpcat3*^{fl/fl} Villin-Cre (IKO) mice fasted overnight and re-fed 60% HFD for 2 hr ($n \geq 5$ /group).

(G) Food intake in *Lpcat3*^{fl/fl} (F/F) and *Lpcat3*^{fl/fl} Villin-Cre (IKO) mice treated with vehicle or GLP-1 receptor antagonist Ex-9 ($n = 3$ /group). Mice were fed 60% HFD and i.p. injected with Ex-9 (5 μ g/25 g BW, twice/day) for 5 days.

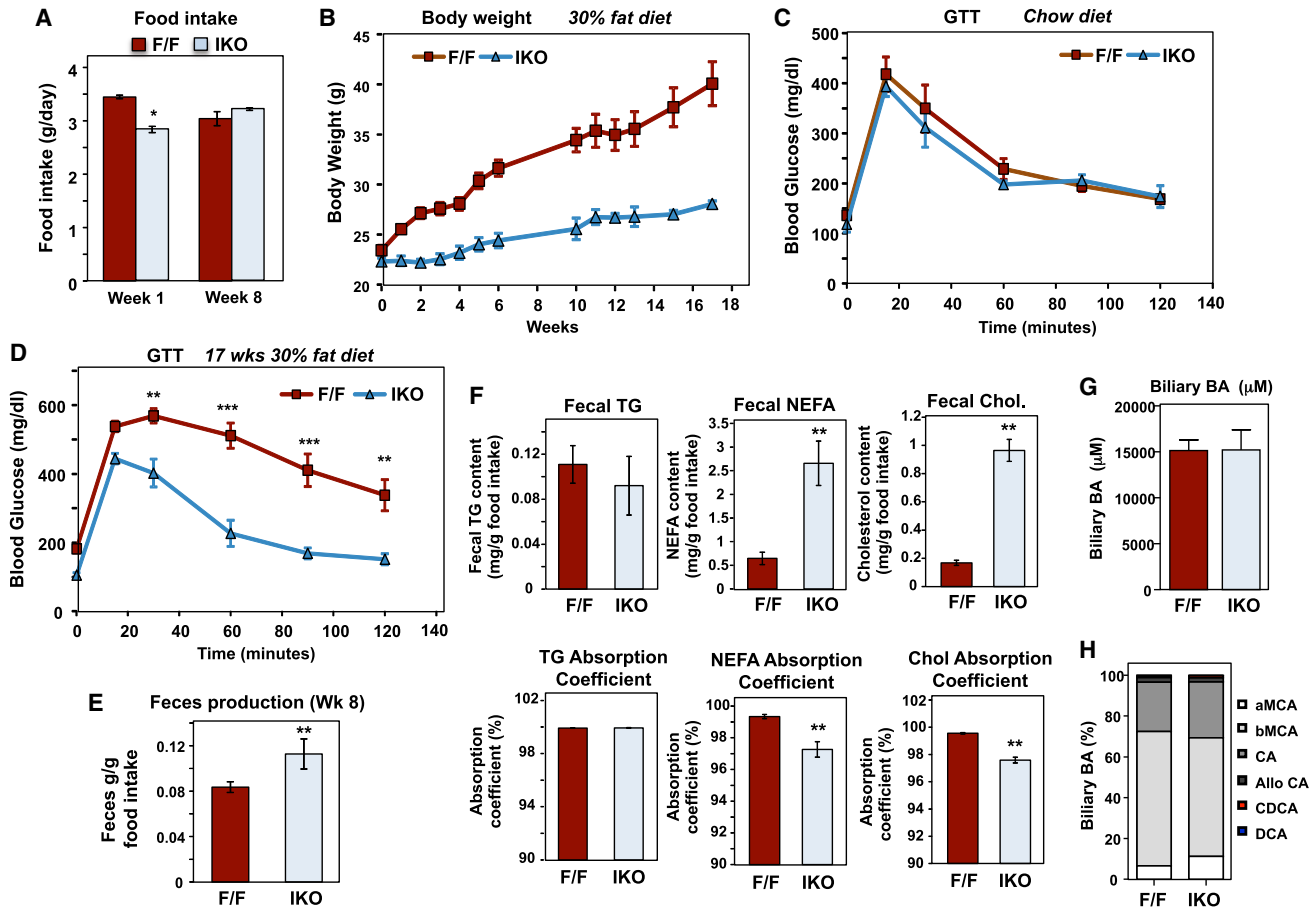
(H) Mass spectrometry analysis of OEA in the serum and jejunum of mice fasted overnight and re-fed 60% HFD ($n \geq 4$ /group). Results from two independent experiments are shown.

Values are means \pm SEM. Statistical analysis was performed with two-way ANOVA (A–C, E, and G), one-way ANOVA (D), and Student's *t* test (F and H). * $p < 0.05$, ** $p < 0.01$, *** $p < 0.001$, not shown, not significant.

intake in fasted mice via activation of cannabinoid type-1 (CB1) receptors (Soria-Gómez et al., 2014). Quantitation by mass spectrometry revealed that OEA levels were significantly increased in the serum and jejunum of HFD-refed IKO mice compared to controls (Figure 3H), whereas total NAPE levels were not significantly altered in the intestine and slightly decreased in the serum (Figure S3A). HFD refeeding had no effect on the levels of AEA in the intestine of IKO mice (Figure S3A). Levels of 2-AG were not consistently altered in the serum or intestine of IKO mice (Figures S3A and S3B). These data suggest that OEA may also contribute to the reduced HFD consumption in IKO mice.

Loss of Intestinal *Lpcat3* Protects from Diet-Induced Obesity

Since *Lpcat3* IKO mice thrive on chow (13.5% fat) but cannot tolerate the standard 60% or 40% fat-content diets commonly used to induce obesity in mice, we tested their ability to survive on a moderate-fat diet (30% calories from fat, 0.02% cholesterol). Although IKO mice initially consumed less food than controls when switched to this diet, they appeared to adapt, as their food intake was comparable to controls after several weeks of feeding (Figure 4A). Despite similar food consumption, however, *Lpcat3* IKO mice gained much less body weight after 17 weeks of feeding (Figure 4B). Diet-induced obesity is



frequently accompanied by glucose intolerance. There was no difference in glucose tolerance between control and *Lpcat3* IKO mice maintained on chow diet (Figure 4C), but *Lpcat3* IKO mice showed improved glucose tolerance compared to controls when maintained on moderate-fat (30%) diet (Figure 4D).

To investigate potential mechanisms underlying the protection from diet-induced obesity in *Lpcat3* IKO mice, we assessed lipid absorption by measuring fecal lipid content. IKO mice produced 35% more feces per gram of food intake than controls (Figure 4E). Furthermore, fecal NEFA and cholesterol levels were 4- to 5-fold higher in IKO mice (Figure 4F). Absorption coefficients for NEFA and cholesterol in *Lpcat3* IKO mice were reduced compared to control mice, suggesting malabsorption of NEFA and cholesterol. By contrast, fecal TG levels were negligible in both groups, and no difference in the TG absorption coefficient was observed, indicating that loss of *Lpcat3* does not impair hydrolysis of ingested TG. Consistent with this observa-

tion, there was no difference in biliary-bile acid levels or bile-acid composition between control and IKO mice (Figures 4G and 4H). Fecal lipid content was also higher in the IKO mice fed western diet (Figure S4).

Lpcat3 Deficiency in Intestine Impairs Fat Absorption and Chylomicron Secretion

To directly test if *Lpcat3* activity was required for transport of dietary fat absorption into the circulation, we performed postprandial TG response assays. Serum-TG levels were dramatically reduced in IKO mice following an intragastric olive-oil load (Figure 5A). We also measured plasma lipid levels in mice fasted overnight and then refed with 60% HFD for 2 hr. This challenge revealed 70% and 25% decreases in serum TG and cholesterol, respectively, in IKO compared to control mice (Figure 5B). In contrast, serum NEFA levels were 2-fold higher in IKO mice. Histological analysis of refed intestines showed an almost complete

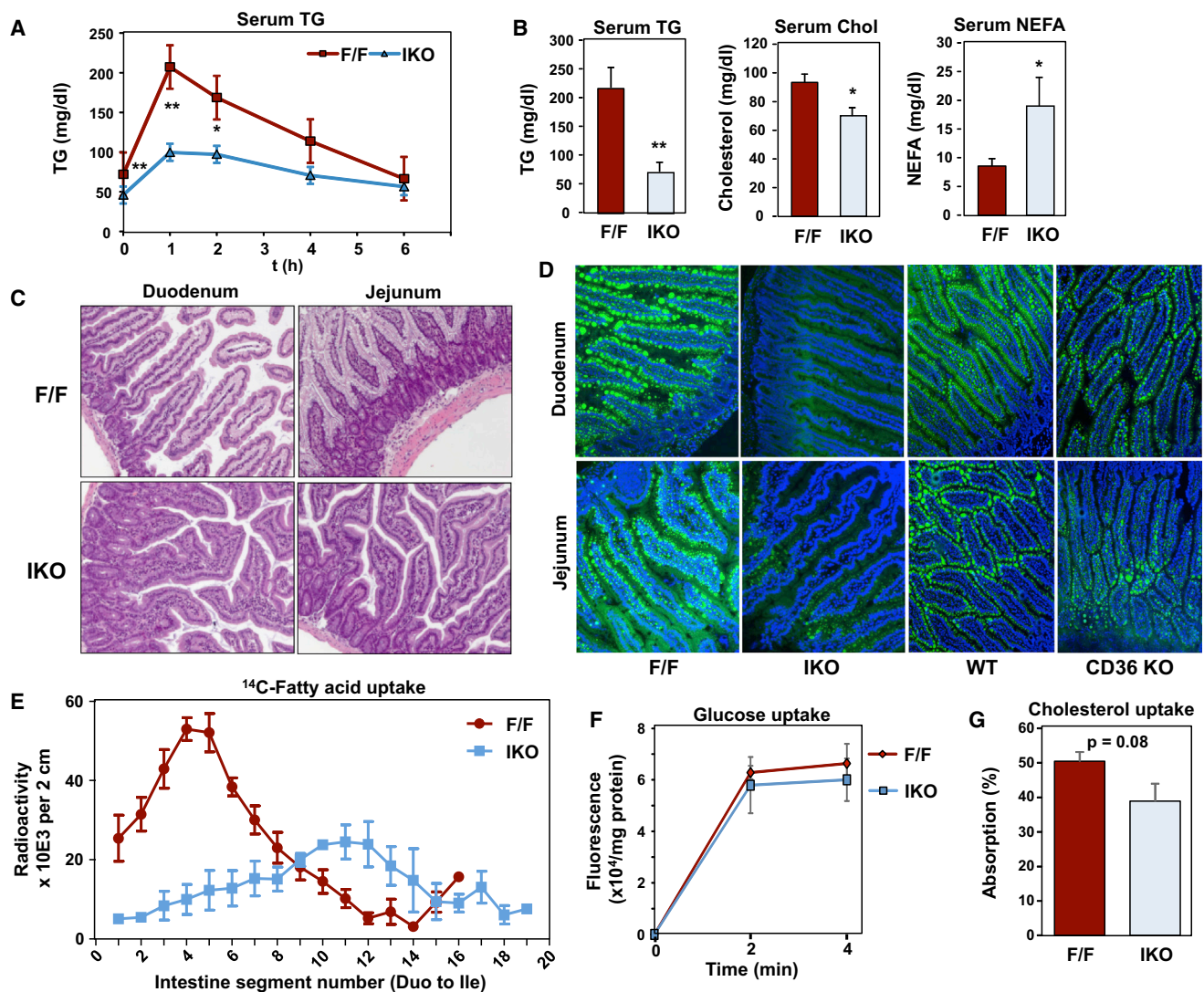


Figure 5. Impaired TG Absorption in *Lpcat3* IKO Mice

(A) Postprandial TG response in male *Lpcat3*^{fl/fl} (F/F) and *Lpcat3*^{fl/fl} Villin-Cre (IKO) mice after oral gavage with olive oil (10 μ l/g BW) (n = 6/group).

(B) Plasma lipid levels in chow-diet-fed male *Lpcat3*^{fl/fl} (F/F) and *Lpcat3*^{fl/fl} Villin-Cre (IKO) mice after fasting overnight and refeeding 60% HFD for 2 hr (n \geq 4/group).

(C) H&E staining of intestine sections from *Lpcat3*^{fl/fl} (F/F) and *Lpcat3*^{fl/fl} Villin-Cre (IKO) mice shown in (B).

(D) Fluorescence images of small intestines of *Lpcat3*^{fl/fl} (F/F) and *Lpcat3*^{fl/fl} Villin-Cre (IKO) mice, and wild-type C57BL/6 and *Cd36*^{-/-} mice after oral gavage with olive oil containing BODIPY-labeled FA for 2 hr.

(E) Distribution of radioactivity in intestinal segments of male *Lpcat3*^{fl/fl} (F/F) and *Lpcat3*^{fl/fl} Villin-Cre (IKO) mice after an oral challenge of olive oil containing ¹⁴C-trioleoylglycerol for 2 hr (n = 3/group).

(F) Ex vivo glucose uptake assay in *Lpcat3*^{fl/fl} (F/F) and *Lpcat3*^{fl/fl} Villin-Cre (IKO) intestines (n = 3/group).

(G) In vivo cholesterol absorption measured by fecal dual-isotope ratio method (n = 4/group).

Values are means \pm SEM. Statistical analysis was performed with two-way ANOVA (A and F) and Student's t test (B and G). *p < 0.05, **p < 0.01.

absence of lipid accumulation in enterocytes of *Lpcat3* IKO duodenum and jejunum, whereas controls contained many lipid droplets (Figure 5C). A similar phenomenon was observed in intestines of IKO mice gavaged with olive oil (Figure S5). These findings suggested that FA uptake, TG synthesis, and/or chylomicron secretion was markedly reduced in *Lpcat3*-deficient enterocytes.

To directly visualize FA uptake into enterocytes, we gavaged mice with BODIPY-labeled FA together with olive oil and exam-

ined enterocytes by microscopy. Abundant fluorescently labeled lipid droplets were observed in control intestines, while almost no fluorescence was present in IKOs (Figure 5D), indicative of a major defect in FA absorption. We also assessed FA uptake in mice deficient in *Cd36* (Chen et al., 2001; Nassir et al., 2007). Although there was a subtle decrease in fluorescence signal in *Cd36* KO enterocytes compared to wild-type controls, loss of *Lpcat3* had a much more severe impact (Figure 5D). Furthermore, analysis of intestinal uptake of radiolabeled FA in

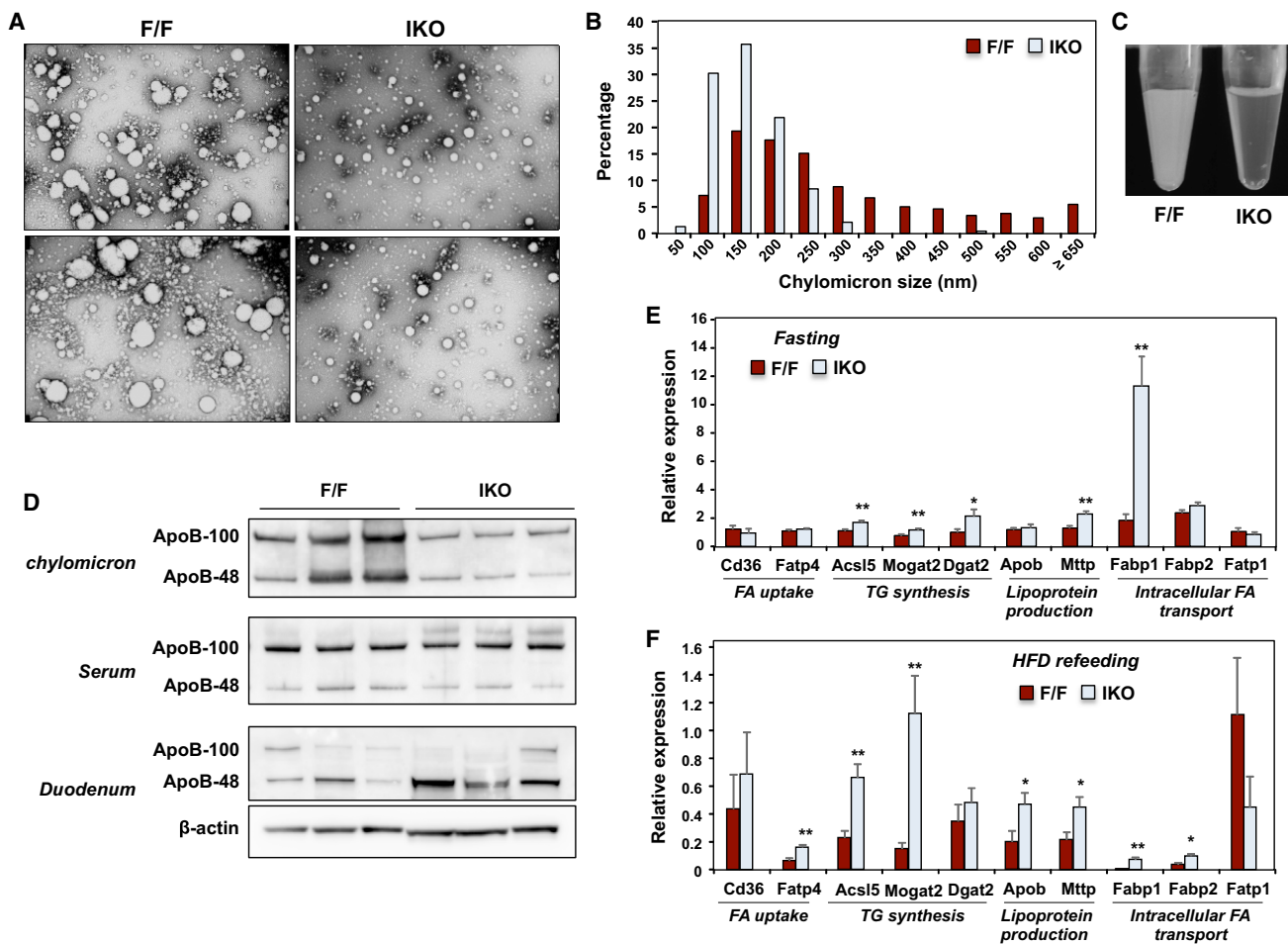


Figure 6. Loss of *Lpcat3* in Intestine Impairs Chylomicron Lipidation and Secretion

(A) Plasma-chylomicron particle size in *Lpcat3*^{fl/fl} (F/F) and *Lpcat3*^{fl/fl} *Villin-Cre* (IKO) mice. Mice were fasted overnight and refed 60% HFD for 2 hr. Chylomicrons were isolated and pooled from five mice/group. Chylomicrons were stained with 2.0% uranyl acetate and visualized by electron microscopy.

(B) Quantification of chylomicron particle size in (A).

(C) Representative pictures of plasma collected from *Lpcat3*^{fl/fl} (F/F) and *Lpcat3*^{fl/fl} *Villin-Cre* (IKO) mice as in (A).

(D) ApoB western blot in chylomicron, whole serum, and duodenum of *Lpcat3*^{fl/fl} (F/F) and *Lpcat3*^{fl/fl} *Villin-Cre* (IKO) mice as in (A).

(E and F) Gene expression in jejunum of *Lpcat3*^{fl/fl} (F/F) and *Lpcat3*^{fl/fl} *Villin-Cre* (IKO) mice during fasting (E) and 60% HFD-refeeding (F) mice ($n \geq 4$ /group). Values are means \pm SEM. Statistical analysis was performed with Student's t test. * $p < 0.05$, ** $p < 0.01$.

response to oral dosing of ¹⁴C-trioleoylglycerol revealed markedly reduced absorption in the proximal intestine of IKO mice and a compensatory shift in uptake to more distal segments (Figure 5E). To determine if absorption defect in IKO mice was specific for FAs, we assessed in vivo cholesterol uptake and ex vivo glucose uptake. There was no difference in labeled glucose uptake between control and IKO intestines (Figure 5F). Cholesterol absorption measured by the fecal dual-isotope ratio method revealed a trend toward decreased uptake in IKO mice (Figure 5G). These observations indicate that not all metabolite transport pathways are compromised in the IKO mice and that the uptake of FAs, and to a lesser degree cholesterol, into enterocytes is preferentially affected.

We next investigated if intestinal *Lpcat3* deficiency affects chylomicron assembly and secretion. Negative staining of plasma chylomicron fractions by electron microscopy (EM) revealed markedly smaller chylomicron particles in *Lpcat3* IKO mice

compared to controls (Figures 6A and 6B), suggesting poor apoB lipidation. Consistent with reduced plasma TG levels and smaller chylomicron particle size, the plasma collected from *Lpcat3*-deficient mice was transparent, while control plasma was milky after HFD refeeding (Figure 6C). ApoB in the chylomicron fraction was decreased in *Lpcat3* IKO mice, whereas total serum apoB was similar (Figure 6D). Together with increased apoB-48 in the duodenum of IKO mice (Figure 6D), these data indicate that chylomicron secretion is impaired in the setting of *Lpcat3* deficiency (Figure 6D). Similar results were obtained in HFD-fed mice (Figure S6). These findings are consistent with the reduced serum levels of TG and cholesterol in IKO mice (Figure 1).

Regulation of Intestinal-Membrane Fluidity Gates FA Uptake

To begin to explore mechanisms underlying defective lipid uptake and chylomicron production, we analyzed the expression

of genes involved in FA uptake, TG synthesis, lipoprotein production, and intracellular FA transport. mRNA levels of most genes implicated in these processes were not reduced, and levels of some were actually increased in *Lpcat3* IKO mice compared to controls in both the fasting and re-fed states (Figures 6E and 6F). Thus, defects in lipid metabolic gene expression could not explain the phenotypes of IKO mice.

To gain insight into how the enzymatic activity of *Lpcat3* was linked to these phenotypes, we performed lipidomic analyses. Previous studies have shown that *Lpcat3* is uniquely required for the incorporation of arachidonate into phospholipids in liver but that its loss does not affect the total abundance of PC (Rong et al., 2015). There was no difference in total levels of PC in enterocytes isolated from *Lpcat3* IKO and control mice (Figure S7A). However, mass spectrometry analysis of individual PC species in chow-diet-fed enterocytes revealed a selective decrease in 34:2 PC (predominantly species containing 16:0 and 18:2 acyl chains) abundance (Figure 7A). There was also a compensatory increase in the abundance of several PC species containing monounsaturated 18:1 chains. In contrast to prior results with the liver-specific *Lpcat3* knockouts (Rong et al., 2015), there was only a small decrease in 38:4 PC (predominantly species containing 18:0 and 20:4 chains) abundance, perhaps reflecting the low abundance of arachidonoyl PC in enterocytes. Feeding the IKO and control mice a 60% HFD for 5 days uncovered more dramatic differences in the abundance linoleoyl and arachidonoyl PC species (Figure S7B). Total PC levels were again not different between groups (Figure S7C).

Next, we tested whether loss of *Lpcat3* would alter the phospholipid composition of chylomicrons secreted from the intestine. Indeed, analysis of PC species in pooled chylomicron fractions isolated from mice gavaged with an olive oil bolus revealed a selective reduction in 34:2 PC (predominantly species containing 16:0 and 18:2 acyl chains) abundance in IKO chylomicrons (Figure S7D). Interestingly, the abundance of individual PC species in the livers of HFD-fed IKO mice also resembled their abundance in the enterocytes, even though *Lpcat3* activity was intact in these livers (Figures S7E and S7F). These findings suggest that the PC composition of the liver is at least in part dependent on intestinal *Lpcat3* activity.

To further address whether changes in enterocyte FA content or phospholipid composition were linked to the weight-loss phenotype, we administered soy PC (63% 18:2-containing PC) or hydro soy PC (88.6% 18:0-containing PC) to IKO mice by oral gavage and monitored food intake and body weight. These diets would be expected to deliver increased levels of either 18:2 or 18:0 FAs to the intestinal epithelium, as PC is hydrolyzed by pancreatic phospholipase A2 to liberate FAs and lysoPC. However, once liberated, the 18:2 would be unable to be reincorporated into PC in mice lacking *Lpcat3*. Neither diet was able to rescue body weight or food intake in the IKO mice (Figures S7G and S7H), consistent with the hypothesis that the change in phospholipids, rather than loss of polyunsaturated FAs, is the cause of the phenotype.

To understand how changes in enterocyte-membrane phospholipid composition might lead to reduced lipid uptake, we performed biophysical studies of lipid movement in intestinal tissue *ex vivo* using live-cell imaging and laurdan staining. Laurdan is a fluorescent lipophilic molecule that can incorporate into mem-

branes, sense the polarity of the membrane environment, and thus detect changes in membrane dynamics (Golfetto et al., 2013; Parasassi and Gratton, 1995). Changes in membrane dynamics shift the laurdan emission spectrum, which can be quantified by the generalized polarization (GP). The striking increase in GP (yellow/orange pseudocolor) in enterocytes lacking *Lpcat3* is indicative of membranes with strongly reduced lipid mobility (Figure 7C). Thus, membranes are less dynamic, and their component lipids move less readily, in the absence of *Lpcat3*. In contrast, we did not find obvious differences in the ultrastructure of intestinal microvilli between control and IKO enterocytes by electron microscopy, suggesting that these changes in membrane composition do not grossly deform membrane structure (Figure 7B).

Evidence from isolated cells suggests that a passive transport dominates when the luminal FA concentration is high, but direct tests of this idea in living intestines are lacking. Thus, we reasoned that decreased membrane dynamics due to altered composition in the absence of *Lpcat3* might be associated with impaired FA uptake into enterocytes. Supporting this notion, *ex vivo* fluorescent-FA uptake into enterocytes was 50% lower in IKO intestines compared to controls (Figure 7D). Moreover, administration of 16:0, 20:4 PC to IKO intestines 30 min prior to label administration increased FA uptake to a level comparable to control intestines (Figure 7E). The time frame of this rescue experiment strongly suggests that changes in enterocyte gene and protein expression are not required. In contrast, PC treatment had no effect on glucose uptake (Figure 7F). To further support our hypothesis that *Lpcat3* was affecting passive transport, we performed additional *ex vivo* FA uptake assays at 4°C on ice, a condition under which active transport is inhibited. Compared to floxed intestines, IKO intestines showed a similar reduction in FA uptake at 4°C on ice as that observed at room temperature (Figure 7G). Furthermore, the administration of 16:0, 20:4 PC, but not 16:0, 18:0 PC, also increased FA uptake at 4°C (Figure 7H), indicating that polyunsaturated PC promotes passive FA uptake into cells.

Collectively, these results demonstrate that loss of *Lpcat3* activity in the intestine leads to a selective defect in the ability to incorporate linoleate and arachidonate into phospholipids. This defect leads to marked biophysical changes in the membrane and is associated with impaired passive FA transport into enterocytes.

DISCUSSION

Dietary-lipid absorption is a complex process that involves several steps: intraluminal hydrolysis of dTG, FA and monoacylglycerol uptake, resynthesis of TG, and chylomicron assembly and secretion (Abumrad and Davidson, 2012). Defects in several steps have been shown to affect fat absorption. Poor solubilization of dietary fat in bile-diverted animals greatly reduces fat absorption (Clark and Holt, 1968; Tso et al., 1978). Deficiency of acyl CoA:monoacylglycerol acyltransferase-2, an enzyme involved in TG resynthesis, delays fat absorption (Yen et al., 2009). Loss of microsomal TG transfer protein (Mttp), which is required for chylomicron assembly, also leads to malabsorption (Xie et al., 2006). In addition, PC has long been recognized to facilitate dietary-lipid uptake, and studies in rats with bile fistulas

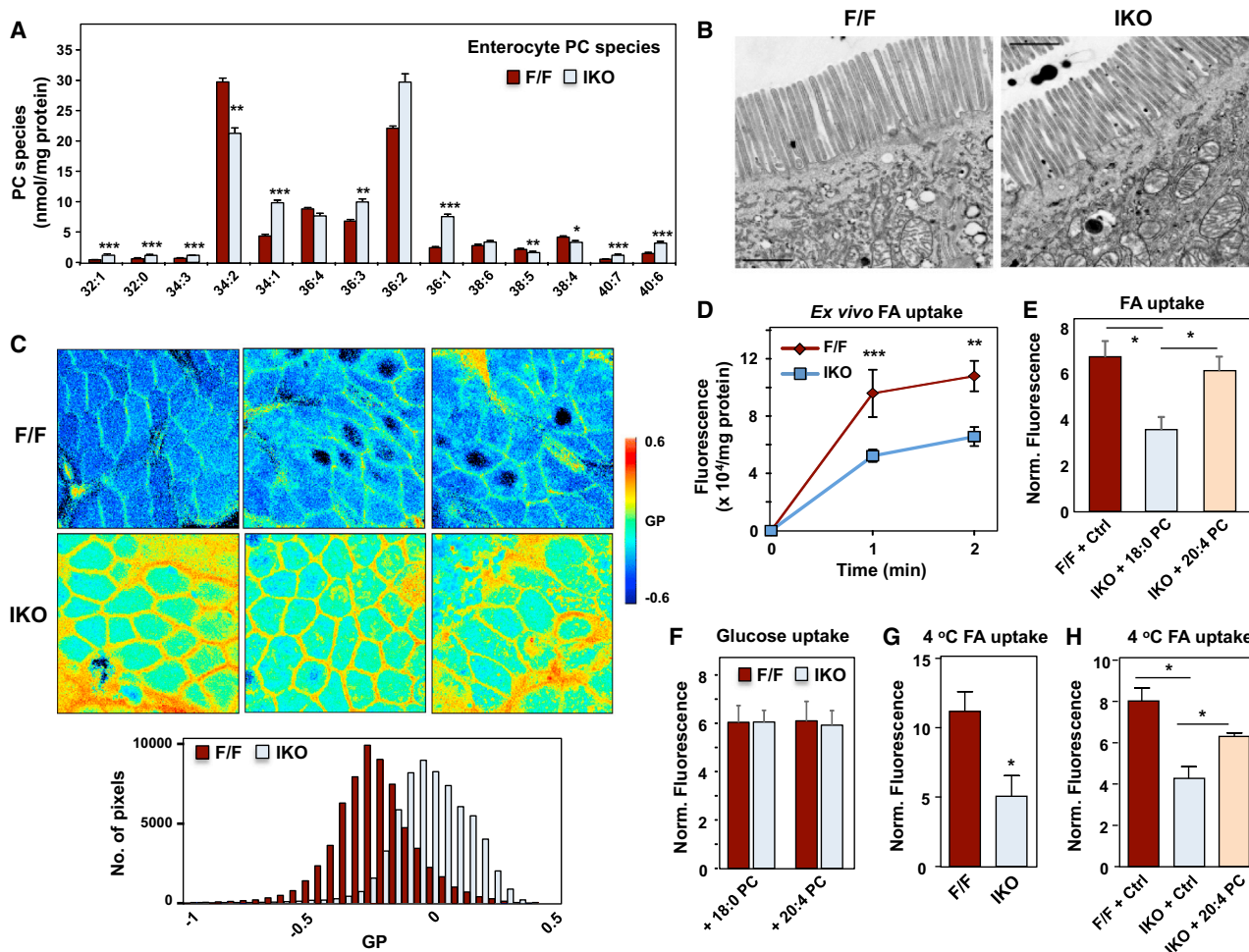


Figure 7. Lpcat3 Deficiency Impairs Linoleate Incorporation and Reduces Enterocyte Membrane Dynamics

(A) ESI-MS/MS analysis of the abundance of PC species in enterocytes from male *Lpcat3^{fl/fl}* (F/F) and *Lpcat3^{fl/fl} Villin-Cre* (IKO) mice fed chow diet ($n \geq 5$ /group). (B) Electron microscopy analysis of microvilli of enterocytes from *Lpcat3^{fl/fl}* (F/F) and *Lpcat3^{fl/fl} Villin-Cre* (IKO) mice.

(C) Laurdan imaging of enterocyte membrane dynamics. Duodenum from male *Lpcat3^{fl/fl}* (F/F) and *Lpcat3^{fl/fl} Villin-Cre* (IKO) mice was stained with laurdan. The laurdan emission spectrum was captured by a 2-photon laser-scan microscope. Generalized polarization (GP) was calculated from the emission intensities obtained from images. Higher GP value indicates that membranes are more ordered and less dynamic. The GP value of each pixel was used to generate a pseudocolor GP image. The binary histograms of the GP distribution of the GP images were quantified at the bottom ($n = 4$).

(D) Ex vivo FA uptake in duodenum of male *Lpcat3^{fl/fl}* (F/F) and *Lpcat3^{fl/fl} Villin-Cre* (IKO) mice at room temperature. Mice were fasted for 4 hr followed by FA uptake assay as described in the [Experimental Procedures](#) ($n = 5$ /group).

(E) Ex vivo FA uptake in duodenum treated with 16:0; 18:0 PC (control) and 16:0; 20:4 PC at room temperature ($n = 4$ /group).

(F) Ex vivo glucose uptake in duodenum of male *Lpcat3^{fl/fl}* (F/F) and *Lpcat3^{fl/fl} Villin-Cre* (IKO) mice treated with 16:0; 18:0 PC (control) and 16:0; 20:4 PC ($n = 4$ /group) at room temperature ($n = 5$ /group).

(G) Ex vivo FA uptake in duodenum of female *Lpcat3^{fl/fl}* (F/F) and *Lpcat3^{fl/fl} Villin-Cre* (IKO) mice at 4°C on ice ($n = 3$ /group).

(H) Ex vivo FA uptake in duodenum treated with 16:0; 18:0 PC (control) and 16:0; 20:4 PC at 4°C on ice ($n = 3$ /group).

Values are means \pm SEM. Statistical analysis was performed with Student's *t* test (A and G), one-way ANOVA (E and H), and two-way ANOVA (D and F). * $p < 0.05$, ** $p < 0.01$, *** $p < 0.001$.

showed that infusion of PC restored the lymphatic output of TG (Tso et al., 1977, 1981). However, beyond the obvious role of biliary PC in fat solubilization, it is unknown whether specific PC species also impact other steps of fat absorption. We have shown here that loss of *Lpcat3* in intestine reduces the abundance of PC containing linoleate and arachidonate and causes severe fat malabsorption. These findings implicate intestinal PC composition as a major determinant of dietary-lipid uptake.

Our biophysical studies revealed that a reduction in linoleoyl and arachidonoyl PC in *Lpcat3* IKO intestinal membranes, possibly together with an increase in saturated or monosaturated PC, results in a striking decrease in membrane fluidity. Membrane dynamics influence a variety of cellular processes, including transmembrane transport and intracellular vesicle trafficking (Spector and Yorek, 1985). Several steps during fat absorption could potentially be affected by changes in membrane dynamics, including FA transport across the apical membrane

of enterocytes, chylomicron transport from ER to Golgi, and secretion into lymphatic circulation. We find that these steps are indeed profoundly altered in *Lpcat3*-deficient intestine. We observed a reduction in FA and cholesterol uptake, along with reduced chylomicron secretion, manifested by decreased chylomicron apoB and increased intestinal apoB levels. It seems likely that changes in membrane fluidity and dynamics in IKO enterocytes contribute to these defects, but further studies will be needed to establish a causal relationship.

Previously, we reported that *Lpcat3* deficiency in liver leads to reduced arachidonoyl PLs and impaired transfer of TG to VLDL (Rong et al., 2015). Hashidate-Yoshida et al. observed an intestinal TG transport defect in newborn *Lpcat3* global KO pups (Hashidate-Yoshida et al., 2015), which they attributed to severe enterocyte damage, including the loss of microvilli. They proposed that loss of PUFA in PLs changes membrane curvature, impairs TG transport to lipoproteins, and leads to lipid-droplet accumulation and cellular damage. One caveat of global *Lpcat3* KO studies, however, is that the mice are moribund and die within days after birth with multiple systemic defects (Rong et al., 2015; Hashidate-Yoshida et al., 2015). By contrast, the ultrastructure of enterocytes in adult *Lpcat3* IKO mice is preserved and TG does not accumulate in enterocytes. Our data suggest that malabsorption in IKO mice is mainly due to defective FA uptake and impaired intracellular chylomicron metabolism.

Although putative transporters such as *Cd36* and *Fatp4* have been reported to be dispensable for FA uptake into enterocytes (Goudriaan et al., 2002; Nassir et al., 2007), the importance of passive transport under physiological conditions has been difficult to test directly due to the inability to manipulate membrane composition in living animals. Here we demonstrate that altering the enterocyte membrane itself affects FA uptake *in vivo*. Our data suggest that the increased membrane acyl-chain saturation in IKO mice, and the consequent altered membrane dynamics, impedes dietary FA uptake. Acute administration of polyunsaturated PC increased passive FA uptake in *Lpcat3*-deficient intestine without affecting the active transport of glucose, indicating that altered membrane composition *per se* is the proximal cause of the defect. Our data are most consistent with the hypothesis that the increased abundance of polyunsaturated PC in the apical membrane facilitates the flip-flop of FAs into the bilayer. Prior *in vitro* studies have shown that FAs move across membranes spontaneously and rapidly (Brunaldi et al., 2010; Kamp and Hamilton, 1992). Whether or not membrane composition also affects the downstream incorporation of FAs into TGs remains to be determined, but the formation of TG droplets from dietary FA was also severely impaired in the *Lpcat3* IKO mice. Our results provide *in vivo* support for the hypothesis that passive transport of FAs across a permissive enterocyte membrane predominates in the context of bolus lipid challenge *in vivo*.

Interestingly, the phospholipid profile of *Lpcat3* KO enterocytes (decreased 18:2-containing PC, decreased 20:4-containing PC, and increased in 18:1- and 20:3-containing PC) is similar to that previously observed in EFA-deficient mucosa (Christon et al., 1989; Enser and Bartley, 1962; Yurkowski and Walker, 1971). EFA deficiency has been recognized to be associated with fat malabsorption for decades (Clark et al., 1973; Hjelte et al., 1990; Levy et al., 1992; Barnes et al., 1941), but the underlying mechanisms have never been defined. It had been sug-

gested that changes in phospholipid profiles in EFA-deficient intestine may be linked to malabsorption, but there has been no *in vivo* system available to test this idea. Our study provides a plausible explanation for why EFAs are important for fat absorption. It is important to note that *Lpcat3* IKO mice are not globally EFA-deficient; they only lack certain EFAs in phospholipids. Our data suggest that loss of EFA-containing PC could be one possible contributor to malabsorption in EFA deficiency, especially given that most alternative explanations have been ruled out (Werner et al., 2002).

Another unexpected finding of this study was the requirement of *Lpcat3* activity for mice to survive on lipid-rich diets. This unique phenotype appears to result from the combination of ineffective lipid absorption and dramatically reduced food intake. Once switched to a HFD or western diet, *Lpcat3* IKO mice stop eating. They continue to resist eating and rapidly lose body weight, even though they exhibit signs of starvation. Interestingly, the suppression of food intake is dependent on the amount of fat present in the diet. There was no difference in food consumption between IKO mice and controls on chow diet, and they were able to adapt to tolerate a 30% fat diet after several days. These observations suggest that the inability to process dietary fat triggers one or more signals that inhibit food intake in *Lpcat3* IKO mice. The fact that the mice are able to tolerate moderate-fat diet despite their severe FA-uptake defect underscores the enormous absorptive capacity of the intestinal tract. The hyperplasia of the intestinal mucosa in IKO mice also probably helps to partially compensate for the defect.

GLP-1 and PYY were highly induced upon HFD feeding in *Lpcat3* IKO mice. These hormones are secreted from enteroendocrine L-cells in the distal small intestine, most likely in response to luminal FA. It is likely that reduced fat absorption in the duodenum and jejunum of IKO mice results in more FA reaching the ileum, where they trigger the secretion of gut hormones. Our data suggest that the excessive GLP-1 secretion contributes to anorexia in *Lpcat3* KO mice, as a GLP-1 receptor antagonist partially rescued food intake. However, additional pathways must also be at play. High-fat feeding induces the biosynthesis of intestinal NAPE and OEA, which inhibit food intake by activating nuclei in the hypothalamus and peripheral sensory fibers (Provinsi et al., 2014; Rodríguez de Fonseca et al., 2001). In this study, intestinal and serum OEA levels were hyperinduced in HFD-refed IKO mice, suggesting a contribution to the reduced food consumption. However, given the severity of the anorexic response, we speculate that additional, as yet unidentified mediators must also be involved.

In conclusion, these results highlight the critical importance of membrane phospholipid composition and dynamics in determining dietary-lipid diffusion across the intestinal membrane, thereby controlling food consumption during high-fat feeding. Future studies will explore whether manipulating intestinal membrane phospholipid composition could be used as a strategy to modulate hyperlipidemia and diet-induced obesity.

EXPERIMENTAL PROCEDURES

Animal Studies

Lpcat3^{fl/fl} and *Lpcat3^{fl/m}*; *Villin-Cre* mice have been described (Rong et al., 2015). *Cd36^{-/-}* mice were obtained from Jackson Laboratory. All mice were housed

under pathogen-free conditions in a temperature-controlled room with a 12 hr light/dark cycle. Mice were fed chow diet (LabDiet #5001), 60% fat diet (Research Diets #D12492), 30% fat diet (Research Diets #D11072204), western diet (Research Diets #D12079), or 1.25% cholesterol diet (Research Diets #C12826). All experiments were performed with male mice unless otherwise stated. Small intestines were excised and cut into three segments with length ratios of 1:3:2 (corresponding to duodenum, jejunum, and ileum). Intestine tissues were frozen in liquid nitrogen and stored at -80°C or fixed in 10% formalin. Blood was collected by retro-orbital bleeding, and the plasma was separated by centrifugation. Plasma lipids were measured with the Wako L-Type TG M kit, the Wako Cholesterol E kit, and the Wako HR series NEFA-HR(2) kit. Tissue and fecal lipids were extracted with Folch lipid extraction (Folch et al., 1957) and measured with the same enzymatic kits. Plasma fast protein liquid chromatography (FPLC) lipoprotein profiles were performed in the Lipoprotein Analysis Laboratory at Wake Forest University. Animal experiments were conducted in accordance with the UCLA Animal Research Committee.

Lipid Uptake

We assessed intestinal uptake of dietary fat as described (Yen et al., 2009). Mice were fasted for 4 hr and gavaged with $1\ \mu\text{Ci}$ of ^{14}C -trioleoylglycerol in $200\ \mu\text{l}$ of olive oil. After 2 hr, we excised the small intestine (between the base of the stomach and the cecal junction), flushed it with $0.5\ \text{mM}$ sodium taurocholate in PBS, and cut it into 2-cm segments. Segments were incubated with $500\ \mu\text{l}$ of $1\ \text{N}$ NaOH at 65°C overnight and mixed with ScintiSafe (Fisher Scientific), and scintillation was counted. In vivo cholesterol absorption was determined by fecal dual-isotope ratio as described (Temel et al., 2005). Absorption of dietary lipids was determined by subtracting the amount of each lipid excreted in feces in 72 hr from the amount of lipid ingested (net fat absorption). This quantity was subsequently expressed as a percentage of the amount of total lipids ingested in 72 hr (coefficient of lipid absorption).

Imaging Studies

Mice were fasted for 4 hr and gavaged with BODIPY 500/510 C1, C12 FAs ($2\ \mu\text{g/g}$ body weight; Molecular Probes #D3823), and olive oil ($10\ \mu\text{l/g}$ body weight) for 2 hr. Small intestines were excised and frozen in optimum cutting temperature (OCT). Ten-micrometer sections were cut, mounted with ProLong Diamond Antifade Mountant with DAPI, and examined under fluorescence microscope. For determination of chylomicron size by transmission electron microscopy, mice were fasted overnight and refed 60% HFD for 2 hr. A total of $200\ \mu\text{l}$ pooled plasma from 5 *Lpcat3^{fl/fl}* and *Lpcat3^{fl/fl}; Villin-Cre* mice was overlaid with $600\ \mu\text{l}$ saline and centrifuged at $50,000\ \text{rpm}$ for 5 hr in a TLA 120.2 rotor, and the chylomicron layer was removed. For electron microscopy, $5\ \mu\text{l}$ of the chylomicron fraction was applied to carbon-coated copper grids and stained with 2.0% uranyl acetate for 15 min. Grids were visualized with a JEOL 100CX transmission electron microscope. Particle diameter was measured using ImageJ.

Membrane Dynamics

Membrane dynamics were analyzed as described, with modifications (Golfetto et al., 2013). Briefly, duodenum from *Lpcat3^{fl/fl}* and *Lpcat3^{fl/fl}; Villin-Cre* mice was excised, cut open, and incubated with $0.15\ \text{mM}$ laurdan (6-dodecanoyl-2-dimethylaminonaphthalene; Invitrogen) at 37°C for 30 min. Tissues were rinsed with phosphate-buffered saline (PBS). Spectral data were acquired with a Zeiss LSM 710 META laser scanning microscope coupled to a two-photon Ti:Sapphire laser (Mai Tai, Spectra Physics) producing 80-fs pulses at a repetition of 80 MHz with two different filters: 460/80 nm and 540/50 nm. Spectral data were processed by the SimFCS software (Laboratory for Fluorescence Dynamics). The GP value was calculated for each pixel using the two laurdan intensity images (460/80 nm and 540/50 nm). The GP value of each pixel was used to generate the pseudocolored GP image.

Ex Vivo FA Uptake Assay

Mice were fasted for 4 hr and euthanized with isoflurane. The small intestine was rinsed in situ with PBS. The ends of the duodenal segment ($\sim 5\ \text{cm}$) were clamped with hemostats forceps to make an intestine sac. The sac was filled with QBT FA uptake-assay solution mixed with $10\ \text{mM}$ sodium taurocholate and $4\ \text{mM}$ oleic acid. The sac was incubated with uptake-assay solution for 1 and 2 min either at room temperature or at 4°C on ice. After in-

cupation, the sac was removed and immediately immersed in ice-cold $0.5\ \text{mM}$ sodium taurocholate in PBS to stop the reaction. The sac was washed twice with $0.5\ \text{mM}$ sodium taurocholate in PBS and scraped with a glass slide to obtain villi, which were further washed twice with $0.5\ \text{mM}$ sodium taurocholate and homogenized with RIPA buffer. Fluorescence signal in the supernatant was read using a fluorescence plate reader with an excitation wavelength of 485 nm and an emission wavelength of 515 nm. Fluorescence was normalized to protein concentration. For PC treatment, intestinal sacs were filled with $25\ \mu\text{M}$ 16:0; 18:0 control or 16:0; 20:4 PC liposomes and incubated in PBS for 30 min. After incubation, intestines were washed with PBS followed prior to assessment of FA uptake.

Statistical Analysis

For all studies, results from quantitative experiments were expressed as means \pm SEM. Where appropriate, significance was calculated by Student's *t* test or one- or two-way ANOVA using Bonferroni multiple comparison.

SUPPLEMENTAL INFORMATION

Supplemental Information includes Supplemental Experimental Procedures and seven figures and can be found with this article online at <http://dx.doi.org/10.1016/j.cmet.2016.01.001>.

AUTHOR CONTRIBUTIONS

B.W., X.R., M.A.D., D.J.H., P.N.H., J.S.W., and T.Q.V. performed experiments. B.W., X.R., D.J.H., P.N.H., J.S.W., B.F.C., E.G., D.A.F., and P.T. designed experiments. P.T., B.W., and D.A.F. wrote the paper.

ACKNOWLEDGMENTS

We thank Jinkuk Choi, Ito Ayaka, and Diana Shih for technical support. We thank Stephen Young, Karen Reue, and Peter Edwards for helpful discussions. This work was supported by grants HL090553, DK063491, DK099810, HL030568, HL074214, GM103540, and GM076516 and AHA Fellowship 13PRE17150049. P.T. is an Investigator of the Howard Hughes Medical Institute.

Received: August 25, 2015

Revised: November 2, 2015

Accepted: December 30, 2015

Published: January 28, 2016

REFERENCES

- Abumrad, N.A., and Davidson, N.O. (2012). Role of the gut in lipid homeostasis. *Physiol. Rev.* **92**, 1061–1085.
- Begg, D.P., and Woods, S.C. (2013). The endocrinology of food intake. *Nat. Rev. Endocrinol.* **9**, 584–597.
- Brunaldi, K., Huang, N., and Hamilton, J.A. (2010). Fatty acids are rapidly delivered to and extracted from membranes by methyl-beta-cyclodextrin. *J. Lipid Res.* **51**, 120–131.
- Camilleri, M. (2015). Peripheral mechanisms in appetite regulation. *Gastroenterology* **148**, 1219–1233.
- Chen, M., Yang, Y., Braunstein, E., Georgeson, K.E., and Harmon, C.M. (2001). Gut expression and regulation of FAT/CD36: possible role in fatty acid transport in rat enterocytes. *Am. J. Physiol. Endocrinol. Metab.* **281**, E916–E923.
- Chow, S.L., and Hollander, D. (1979). Linoleic acid absorption in the unanesthetized rat: mechanism of transport and influence of luminal factors on absorption. *Lipids* **14**, 378–385.
- Christon, R., Even, V., Daveloose, D., Léger, C.L., and Viret, J. (1989). Modification of fluidity and lipid-protein relationships in pig intestinal brush-border membrane by dietary essential fatty acid deficiency. *Biochim. Biophys. Acta* **980**, 77–84.
- Clark, S.B., and Holt, P.R. (1968). Rate-limiting steps in steady-state intestinal absorption of triolein-1- ^{14}C . Effect of biliary and pancreatic flow diversion. *J. Clin. Invest.* **47**, 612–623.

- Clark, S.B., Ekkers, T.E., Singh, A., Balint, J.A., Holt, P.R., and Rodgers, J.B., Jr. (1973). Fat absorption in essential fatty acid deficiency: a model experimental approach to studies of the mechanism of fat malabsorption of unknown etiology. *J. Lipid Res.* **14**, 581–588.
- Enser, M., and Bartley, W. (1962). The effect of; essential fatty acid' deficiency on the fatty acid composition of the total lipid of the intestine. *Biochem. J.* **85**, 607–614.
- Folch, J., Lees, M., and Sloane Stanley, G.H. (1957). A simple method for the isolation and purification of total lipides from animal tissues. *J. Biol. Chem.* **226**, 497–509.
- Fu, J., Gaetani, S., Oveysi, F., Lo Verme, J., Serrano, A., Rodríguez De Fonseca, F., Rosengarth, A., Luecke, H., Di Giacomo, B., Tarzia, G., and Piomelli, D. (2003). Oleylethanolamide regulates feeding and body weight through activation of the nuclear receptor PPAR- α . *Nature* **425**, 90–93.
- Gillum, M.P., Zhang, D., Zhang, X.M., Erion, D.M., Jamison, R.A., Choi, C., Dong, J., Shanabrough, M., Duenas, H.R., Frederick, D.W., et al. (2008). N-acylphosphatidylethanolamine, a gut-derived circulating factor induced by fat ingestion, inhibits food intake. *Cell* **135**, 813–824.
- Golfetto, O., Hinde, E., and Gratton, E. (2013). Laurdan fluorescence lifetime discriminates cholesterol content from changes in fluidity in living cell membranes. *Biophys. J.* **104**, 1238–1247.
- Goudriaan, J.R., Dahlmans, V.E., Febbraio, M., Teusink, B., Romijn, J.A., Havekes, L.M., and Voshol, P.J. (2002). Intestinal lipid absorption is not affected in CD36 deficient mice. *Mol. Cell. Biochem.* **239**, 199–202.
- Harmon, C.M., Luce, P., and Abumrad, N.A. (1992). Labelling of an 88 kDa adipocyte membrane protein by sulpho-N-succinimidyl long-chain fatty acids: inhibition of fatty acid transport. *Biochem. Soc. Trans.* **20**, 811–813.
- Hashidate-Yoshida, T., Harayama, T., Hishikawa, D., Morimoto, R., Hamano, F., Tokuoka, S.M., Eto, M., Tamura-Nakano, M., Yanabu-Takanashi, R., Mukumoto, Y., et al. (2015). Fatty acid remodeling by LPCAT3 enriches arachidonate in phospholipid membranes and regulates triglyceride transport. *eLife* **4**, <http://dx.doi.org/10.7554/eLife.06328>.
- Hjelte, L., Melin, T., Nilsson, A., and Strandvik, B. (1990). Absorption and metabolism of [3 H]arachidonic and [14 C]linoleic acid in essential fatty acid-deficient rats. *Am. J. Physiol.* **259**, G116–G124.
- Ho, S.Y., and Storch, J. (2001). Common mechanisms of monoacylglycerol and fatty acid uptake by human intestinal Caco-2 cells. *Am. J. Physiol. Cell Physiol.* **281**, C1106–C1117.
- Kamp, F., and Hamilton, J.A. (1992). pH gradients across phospholipid membranes caused by fast flip-flop of un-ionized fatty acids. *Proc. Natl. Acad. Sci. USA* **89**, 11367–11370.
- Levy, E., Garofalo, C., Thibault, L., Dionne, S., Daoust, L., Lepage, G., and Roy, C.C. (1992). Intraluminal and intracellular phases of fat absorption are impaired in essential fatty acid deficiency. *Am. J. Physiol.* **262**, G319–G326.
- Ling, K.Y., Lee, H.Y., and Hollander, D. (1989). Mechanisms of linoleic acid uptake by rabbit small intestinal brush border membrane vesicles. *Lipids* **24**, 51–55.
- Murota, K., and Storch, J. (2005). Uptake of micellar long-chain fatty acid and sn-2-monoacylglycerol into human intestinal Caco-2 cells exhibits characteristics of protein-mediated transport. *J. Nutr.* **135**, 1626–1630.
- Nassir, F., Wilson, B., Han, X., Gross, R.W., and Abumrad, N.A. (2007). CD36 is important for fatty acid and cholesterol uptake by the proximal but not distal intestine. *J. Biol. Chem.* **282**, 19493–19501.
- Nauli, A.M., Nassir, F., Zheng, S., Yang, Q., Lo, C.M., Vonlehmden, S.B., Lee, D., Jandacek, R.J., Abumrad, N.A., and Tso, P. (2006). CD36 is important for chylomicron formation and secretion and may mediate cholesterol uptake in the proximal intestine. *Gastroenterology* **131**, 1197–1207.
- Parasassi, T., and Gratton, E. (1995). Membrane lipid domains and dynamics as detected by Laurdan fluorescence. *J. Fluoresc.* **5**, 59–69.
- Provensi, G., Coccorello, R., Umehara, H., Munari, L., Giacovazzo, G., Galeotti, N., Nosi, D., Gaetani, S., Romano, A., Moles, A., et al. (2014). Satiety factor oleylethanolamide recruits the brain histaminergic system to inhibit food intake. *Proc. Natl. Acad. Sci. USA* **111**, 11527–11532.
- Barnes, R.H., Miller, E.S., and Burr, G.O. (1941). Fat absorption in essential fatty acid deficiency. *J. Biol. Chem.* **140**, 773–778.
- Rodríguez de Fonseca, F., Navarro, M., Gómez, R., Escuredo, L., Nava, F., Fu, J., Murillo-Rodríguez, E., Giuffrida, A., LoVerme, J., Gaetani, S., et al. (2001). An anorexic lipid mediator regulated by feeding. *Nature* **414**, 209–212.
- Rong, X., Albert, C.J., Hong, C., Duerr, M.A., Chamberlain, B.T., Tarling, E.J., Ito, A., Gao, J., Wang, B., Edwards, P.A., et al. (2013). LXRs regulate ER stress and inflammation through dynamic modulation of membrane phospholipid composition. *Cell Metab.* **18**, 685–697.
- Rong, X., Wang, B., Dunham, M.M., Hedde, P.N., Wong, J.S., Gratton, E., Young, S.G., Ford, D.A., and Tontonoz, P. (2015). Lpcat3-dependent production of arachidonoyl phospholipids is a key determinant of triglyceride secretion. *eLife* **4**, <http://dx.doi.org/10.7554/eLife.06557>.
- Schwartz, G.J., Fu, J., Astarita, G., Li, X., Gaetani, S., Campolongo, P., Cuomo, V., and Piomelli, D. (2008). The lipid messenger OEA links dietary fat intake to satiety. *Cell Metab.* **8**, 281–288.
- Shim, J., Moulson, C.L., Newberry, E.P., Lin, M.H., Xie, Y., Kennedy, S.M., Miner, J.H., and Davidson, N.O. (2009). Fatty acid transport protein 4 is dispensable for intestinal lipid absorption in mice. *J. Lipid Res.* **50**, 491–500.
- Skála, I., and Konrádová, V. (1969). Hypertrophy of the small intestine after its partial resection in the rat. Ultrastructure of the intestinal epithelium. *Am. J. Dig. Dis.* **14**, 182–188.
- Soria-Gómez, E., Bellocchio, L., Reguero, L., Lepousez, G., Martin, C., Bendahmane, M., Ruehle, S., Remmers, F., Desprez, T., Matias, I., et al. (2014). The endocannabinoid system controls food intake via olfactory processes. *Nat. Neurosci.* **17**, 407–415.
- Spector, A.A., and Yorek, M.A. (1985). Membrane lipid composition and cellular function. *J. Lipid Res.* **26**, 1015–1035.
- Stahl, A., Hirsch, D.J., Gimeno, R.E., Punreddy, S., Ge, P., Watson, N., Patel, S., Kotler, M., Raimondi, A., Tartaglia, L.A., and Lodish, H.F. (1999). Identification of the major intestinal fatty acid transport protein. *Mol. Cell* **4**, 299–308.
- Temel, R.E., Lee, R.G., Kelley, K.L., Davis, M.A., Shah, R., Sawyer, J.K., Wilson, M.D., and Rudel, L.L. (2005). Intestinal cholesterol absorption is substantially reduced in mice deficient in both ABCA1 and ACAT2. *J. Lipid Res.* **46**, 2423–2431.
- Trotter, P.J., Ho, S.Y., and Storch, J. (1996). Fatty acid uptake by Caco-2 human intestinal cells. *J. Lipid Res.* **37**, 336–346.
- Tso, P., Balint, J.A., and Simmonds, W.J. (1977). Role of biliary lecithin in lymphatic transport of fat. *Gastroenterology* **73**, 1362–1367.
- Tso, P., Lam, J., and Simmonds, W.J. (1978). The importance of the lysophosphatidylcholine and choline moiety of bile phosphatidylcholine in lymphatic transport of fat. *Biochim. Biophys. Acta* **528**, 364–372.
- Tso, P., Kendrick, H., Balint, J.A., and Simmonds, W.J. (1981). Role of biliary phosphatidylcholine in the absorption and transport of dietary triolein in the rat. *Gastroenterology* **80**, 60–65.
- Tso, P., Nauli, A., and Lo, C.M. (2004). Enterocyte fatty acid uptake and intestinal fatty acid-binding protein. *Biochem. Soc. Trans.* **32**, 75–78.
- Werner, A., Minich, D.M., Havinga, R., Bloks, V., Van Goor, H., Kuipers, F., and Verkade, H.J. (2002). Fat malabsorption in essential fatty acid-deficient mice is not due to impaired bile formation. *Am. J. Physiol. Gastrointest. Liver Physiol.* **283**, G900–G908.
- Xie, Y., Newberry, E.P., Young, S.G., Robine, S., Hamilton, R.L., Wong, J.S., Luo, J., Kennedy, S., and Davidson, N.O. (2006). Compensatory increase in hepatic lipogenesis in mice with conditional intestine-specific Mttp deficiency. *J. Biol. Chem.* **281**, 4075–4086.
- Yen, C.L., Cheong, M.L., Grueter, C., Zhou, P., Moriwaki, J., Wong, J.S., Hubbard, B., Marmor, S., and Farese, R.V., Jr. (2009). Deficiency of the intestinal enzyme acyl CoA:monoacylglycerol acyltransferase-2 protects mice from metabolic disorders induced by high-fat feeding. *Nat. Med.* **15**, 442–446.
- Yurkowski, M., and Walker, B.L. (1971). The molecular species of mucosal phosphatidylcholines from the small intestine of normal and essential fatty acid-deficient rats. *Biochim. Biophys. Acta* **231**, 145–152.